SOLAR RADIATION PREDICTION USING WAVELET DECOMPOSITION

J. P. Coelho[a], J. Boaventura Cunha[b,c] and P.B. De Moura Oliveira[b,c]

a. Instituto Politécnico de Bragança, Escola Superior de Tecnologia e Gestão
5301-854 Bragança, Portugal.
b. Universidade de Trás-os-Montes e Alto Douro, Dep. Engenharias
5001-911 Vila Real, Portugal
c. CITAB – Centro de Investigação e de Tecnologias Agro-Ambientais e Biológicas
5001-911 Vila Real, Portugal
e-mail: jpcoelho@ipb.pt

Abstract: Nowadays, a substantial part of the agricultural production takes place in greenhouses, which enable to tune the crop growing by modifying, artificially, the environmental conditions and the plant's nutrition. The main goal is to optimise the balance between the production economic return and the operation costs of the climate actuators. Severe environment and market restrictions jointly with an increasing tendency of the fuel price motivate the development of more "intelligent" energy regulators. In order to formulate the best options for a production plan, this type of artificial supervisors must be able to formulate close predictions on a large set of variables. Considering, for instance, the air temperature control inside a greenhouse, the system must be able to close predict the evolution of the solar radiation since this is the exogenous variable which most influences the thermal load during the day. In this paper, an artificial neural network, in conjunction with a wavelet decomposition strategy, is used for forecasting, an hour ahead, the instantaneous solar radiation energy density sampled at one minute interval. The results obtained from this work encourage further exploitation of this kind of signal processing technique.

#
Keywords: Time-series prediction, neural networks, wavelet decomposition, AR models.

1. INTRODUCTION

Greenhouses are building structures that allow the creation of an indoor microclimate for crop development. In order to provide the best environmental conditions, this microclimate can be modified by artificial actuations such as: heating, ventilation and CO_2 supply. As one could expect, this non-natural conditions are achieved by additional energy spent in the production. In this context, a regulator which minimises the energy consumption while keeping the state variables as close as possible to the optimum crop physiological response is essential.

State-of-the-art greenhouse climate controllers are based on models to simulate and predict greenhouse environment behaviour (Coelho *et al*., 2005; van Straten, 1996). These models must be able to describe indoor climate process dynamics, which are functions of the control actions taken and the outside climate. Moreover, if predictive or feedforward control techniques are to be applied, it is necessary to employ models to describe and predict the outside climate, being the most relevant air temperature and solar radiation. Concerning this last variable, it is assumed that the dynamic system state space is not directly observable. Hence one will try to catch it's behaviour by fitting it in a time-series structure. In this situation the appropriate response, in a particular time instant, will depend, solely, on past observations.

The overall objective of this study is to predict the solar radiation future trend by taking into consideration only the past observations of the series. In this context several models were tested with a

special focus given to the one which uses a data pre-processing based on the Haar wavelet decomposition.

2. THE HAAR WAVELET

In time-series prediction, wavelets can be used to reduce the data dimensionality, i.e. the original signal is fractioned into several signals with different spectral contents. Afterwards, a set of models is used to predict each of the components. Finally, the partial results achieved are used to obtain the original signal's prediction. Alternatively, in (Mellit *et al.*, 2006) the dilations and translations of Morlet wavelets are used as activation functions in artificial neural networks.

The wavelet transform can be viewed as a filter bank (Strang and Nguyen, 1996). In particular, the Haar Wavelet decomposition of a signal is resumed by it's journey trough a filter bank with high-pass and low-pass profiles. The following figure illustrates this strategy.

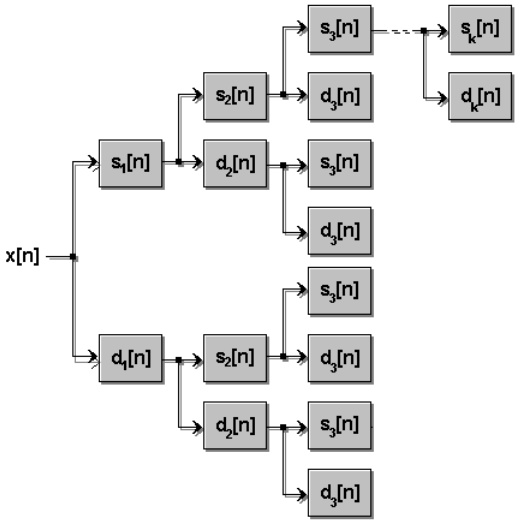

Fig. 1. The Haar Wavelet as a filter bank.

As mentioned previously, in this radial structure coexist two different types of filters with low-pass and a high-pass frequencies responses. The low-pass type impulse response, for a giving filtering depth k, is designated, in Figure 1, by $s_k[n]$. On the other way, the high-pass filter impulse response is represented by $d_k[n]$. In the Haar wavelet context, the filter impulse responses are (Walker, 1999):

$$s[n] = \frac{\delta[n] + \delta[n-1]}{2} \tag{1}$$

$$d[n] = \frac{\delta[n] - \delta[n-1]}{2} \tag{2}$$

Equations (1) and (2) belong to two stable and causal filters. In both equations $\delta[n]$ refers to Kronecker delta and $n \in N$ is related to the sample number.

Applying the Z transform to (1) and (2) results in the following transfer functions:

$$S(z) = \frac{z+1}{2z} \tag{3}$$

$$D(z) = \frac{z-1}{2z} \tag{4}$$

In the following figure the magnitude profile of both frequency responses (the phase plot is neglected since it's linear) are shown.

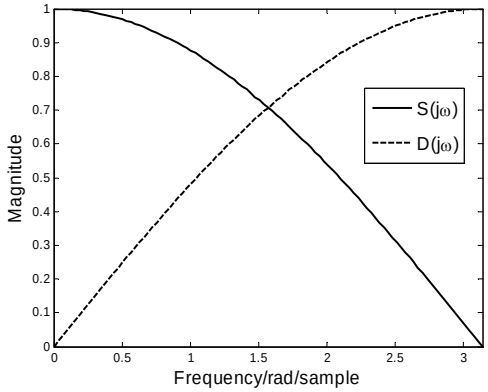

Fig. 2. Frequency response magnitude for the two types network filters.

The convolution of the impulse response $s[n]$ with the signal $x[n]$ results, in a signal composed by the arithmetic mean of consecutive samples. In the same way, when it passes through $d[n]$, $x[n]$ becomes a signal taken as the first difference of the original signal. The result of the low-pass filter can be interpreted as the signal 'tendency'. On the other side the high-pass output refers to the signal 'detail'.

The radial structure presented earlier points out to the possibility of estimating the 'tendency of the tendency' until an arbitrary level k. The filter's impulse response presented in each level can be different as we will see afterwards.

Assuming at this stage, the high-pass filters all alike, the 'tendency of the tendency' of a signal, i.e. the second degree tendency represents the signal filtered by a filter whose impulse response is the convolution of the impulse response on each level:

$$x_2^S[n] = s[n] * s[n] * x[n] \tag{5}$$

Figure 3 shows the frequency response of this cascade structure for five different depth levels. As one could expect, and following the original signal tendency line, the increase of the tree depth implies a filtering with decreased bandwidth. Thus, the partial generated signals dynamics tend to lower down. The same could be stated for the 'detail' part of the signal.

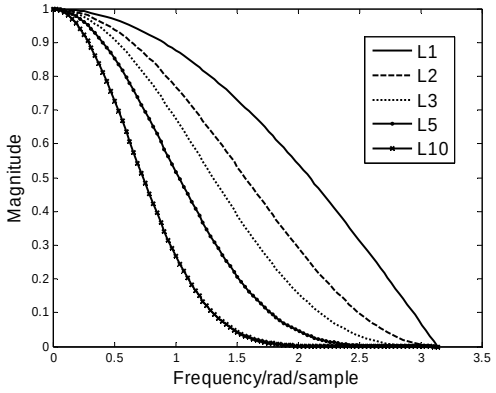

Fig. 3. Frequency response of five different filtering levels.

The bank filter structure shows that it is also possible to estimate the 'detail's tendency' or the 'tendency's detail'. This information results from the passage of the signal $x[n]$ through the band-pass filter with direction dependent profiles.

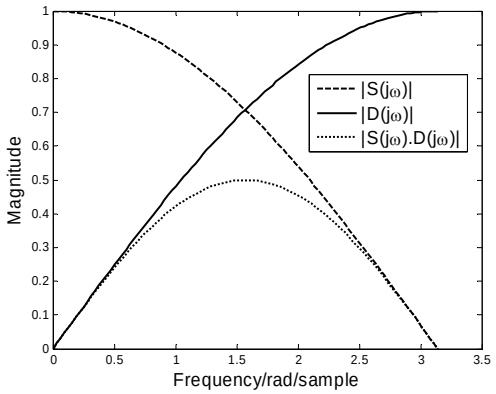

Fig. 4. The 'tendency's detail' as a band-pass filter.

If the bank filters frequency responses are identical, there will be redundancy of information. For instance $S_1(z)\cdot D_2(z)\cdot S_3(z)$ has the same frequency response as $S_1(z)\cdot S_2(z)\cdot D_3(z)$. One of the advantages of this decomposition method is it's reversibility, i.e., it is possible to obtain the original signal back from the 'details' and 'tendencies' computation. For example, since:

$$x[n] = x_1^S[n] + x_1^D[n] \tag{6}$$

with

$$x_1^S[n] = x[n] * s[n] \tag{7}$$

and

$$x_1^D[n] = x[n] * d[n] \tag{8}$$

The following expression is obtained,

$$\begin{aligned} x_1^S[n] + x_1^D[n] &= x[n] * \big(s[n] + d[n]\big) \\ &= x[n] * \left(\frac{\delta[n] + \delta[n-1]}{2} + \frac{\delta[n] - \delta[n-1]}{2}\right) \\ &= x[n] * \delta[n] = x[n] \end{aligned} \tag{9}$$

As stated before the bank filters frequency responses can be different from each other. One common strategy is to use compressed filters spectra forms, that is, filters with zero padding between the two non-zero samples (Soltani, 2002). With this strategy it is possible to have a larger capability in frequency discrimination. For example, the following impulse responses:

$$s_2[n] = \frac{\delta[n] + \delta[n-2]}{2} \tag{10}$$

$$d_2[n] = \frac{\delta[n] - \delta[n-2]}{2} \tag{11}$$

$$s_4[n] = \frac{\delta[n] + \delta[n-4]}{2} \tag{12}$$

$$d_4[n] = \frac{\delta[n] - \delta[n-4]}{2} \tag{13}$$

are obtained by dilations of the "mother" wavelet expressed by equations (1) and (2). The frequency response of these filters is represented in the following figure.

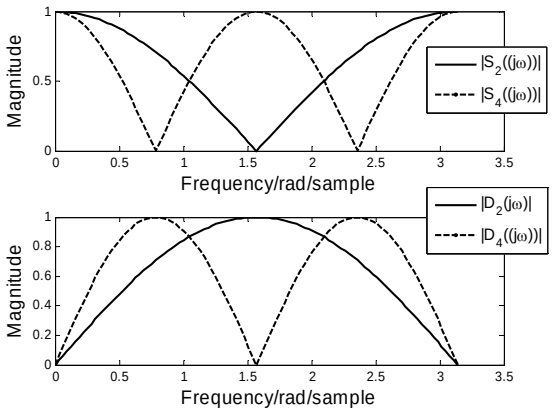

Fig. 6. Frequency response magnitude for dilation versions of initial filters.

It can be shown that, for a k level decomposition, the original signal can be reconstructed by:

$$x[n] = x_k^S[n] + \sum_k x_k^D[n] \tag{14}$$

Let's now consider de solar energy density for a particular cloudy day with the following aspect:

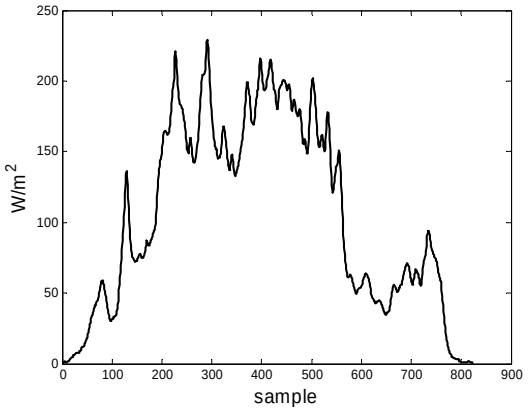

Fig. 7. Solar radiation power density.

This data was acquired, using a pyranometer, with a one minute sampling time. A fourth level Haar decomposition with dyadic frequency response filters of the previous signal leads to four new signals with the following profiles:

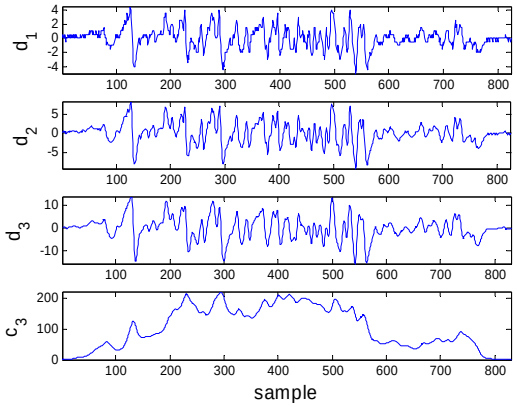

Fig. 8. Wavelet decomposition of the solar radiation density.

It is this information, rather than the raw data itself, that will be feed to a non-linear parametric model.

#

3. SOLAR RADIATION PREDICTION

In this section a comparative study of several types of parametric models will be investigated concerning their ability to predict solar radiation using a sixty steps ahead horizon.

The solar radiation, represented as a time-series, is a very complex prediction problem due to the extremely uncorrelated high frequency components. Although the low-frequency profile could be obtained from a deterministic radiation model, the high-frequency oscillation due to disturbances, such as clouds and atmosphere attenuation, is extremely difficult to predict using only past information. In general, the evolution of the relative prediction error versus the forecast horizon, for a giving time-series model, will show a logarithmic profile with the error rising fast in the first thirty or forty steps ahead as can be seen in fig. 9. The fact that the first derivative of the error is slowing down after this point does not mean that there is advantageous to take predictions farther in time. It only says that there is a smaller margin to make the things worst!

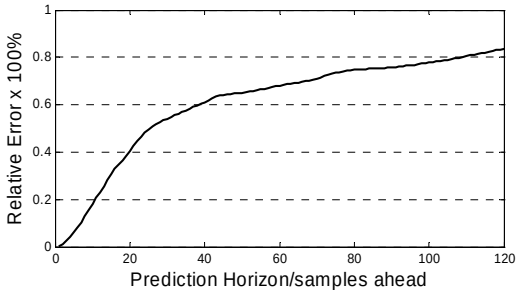

Fig. 9. Prediction error as a prediction horizon function.

In the following items a set of prediction models will be investigated concerning their capacity to close forecast the solar radiation on a highly fluctuating day. The maximum prediction horizon taken is sixty steps ahead and the performance is inferred taking into consideration two indexes: the average of the root-mean squared (RMS) error along the prediction horizon and the percentage of change in direction. The later is a qualitative index that represents the model ability to predict the tendency, i.e. capable of following the signal derivative sign. This figure of merit is very important in the context of air temperature regulation under a model predictive control (MPC), since the heating and ventilation requirements will be computed taking into account if it will be expected a heat load increase or decrease in the near future. Equations for both performance indexes are (15) and (16).

$$J[N] = \frac{1}{N}\sum_{n=0}^{N-H-1}\sqrt{\frac{1}{H}\sum_{k=n}^{n+H}\left(x[k]-\hat{x}[k]\right)^2} \qquad (15)$$

Where N refers to the number of observations, H is the prediction horizon, $\bar{x}$ is the signal average and the pair $\{x[n],\hat{x}[n]\}$ represents the input and predicted signals, respectively.

$$Q[N] = \frac{1}{N}\sum_{n=1}^{N-H-1}\eta[n] \qquad (16)$$

Where,

$$\eta[n] = \sum_{k=n}^{n+H} u\left[\Delta\hat{x}[k]\cdot\Delta x[k]\right] \qquad (17)$$

and $u[\cdot]$ refers to the Heaviside (or discrete step) function.

3.1 A simple AR(10) Model.

In this section the behavior of a simple ten pole filter will be investigated for prediction purposes. The filter coefficients were computed, using the previous day data, by means of a least squares algorithm. The following picture illustrates the model's ability to predict the solar radiation over a time horizon of 1 hour with a time step of 1 minute.

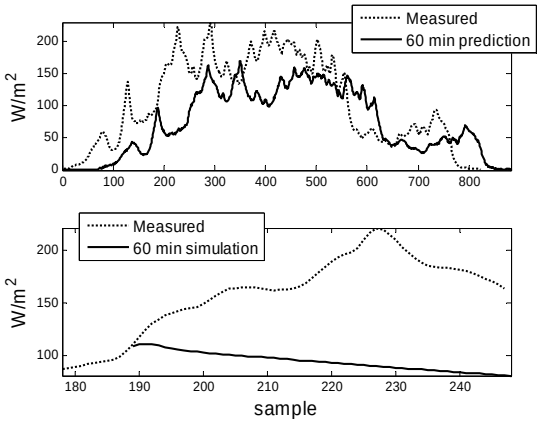

Fig. 10. Top: sixty steps ahead prediction of the solar radiation using an AR(10) model. Bottom: the prediction tendency in a one hour period taken at sample 187.

First of all it seems that the predicted signal is out of phase with the measured one. Indeed, the predicted radiation is lagging the real version by, approximately, the prediction horizon. Figure 10 also shows that the total energy predicted for a day is lower than the measured one. This can be well understood by looking at the filter impulse response illustrated in Fig. 11. After the excitation signal, the response will asymptotically tend to zero as the time passes by. So, in closed-loop, there is no chance to achieve a good dynamic behaviour prediction, especially when the horizon is large and the trend of the signal is upward.

Due to the signal periodic nature, it is always possible to try to use the past day to predict the present one. However, the correlation generally observed between days is only of significant importance for the very low frequency component. The computation of the cross-correlation is not zero for lags out of the narrow interval around zero. But the values obtained only reflect the numeric nature of the algorithm and does not have any meaning in terms of day's interconnection.

Frequently, the rigid nature of these type of models can be seen as a serious drawback due to the low correlation between successive days. In this context often one tries to estimate the filter parameters more closely to each of the prediction start-up point. The recursive version of the least squares method seems tailored to this approach. Figure 12 presents the new prediction based on this strategy.

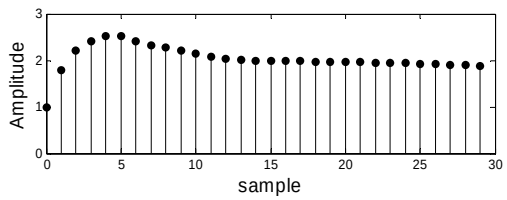

Fig. 11. Filter's impulse response.

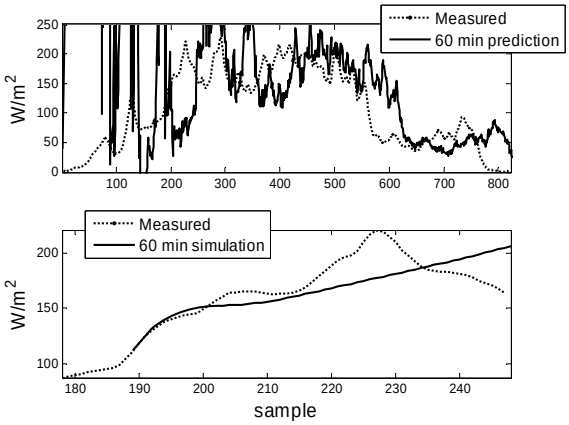

Fig. 12. Prediction results using a recursive AR(10) model: real and predicted values for the sample *k*+60 (top) and simulated values over the prediction horizon time interval starting at sample 187 (bottom).

At first glance the predictions instability suggests an instable model. Indeed, this is what happens as it can be seen by inspection of the following figure.

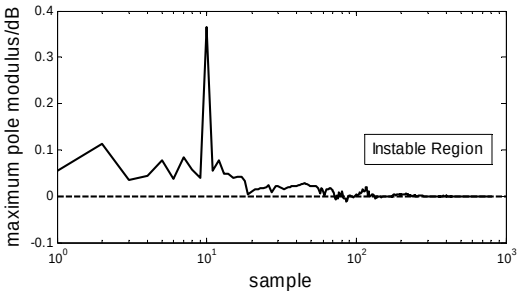

Fig. 13. Stability chart as a function of time.

Relatively to the AR(10) algorithm, the dynamic behaviour is, punctually, improved but the instability, especially for large prediction horizons, tends to make the predictor to 'windup'.

3.2 The Artificial Neural Network.

The previous algorithms tried to express the predicted output as a linear combination of past inputs. The use of artificial neural networks (ANN) can overcome this constraint by trying to relate the past values in a non-linear fashion. Linear basis networks (LBN), as well as radial ones (RBN), applied to time-series prediction are extensively found in literature (Kingdom, 1993) (Ferreira and Ruano, 2004), among many others.

The ANN performance is strongly related to the possibility to find reasonable non-linear relationships between signals. If the signal to predict does not exhibit this type of associations, the results obtained are not far form the ones obtained by simple linear models. The following figure presents the prediction and simulation results obtained by a LBN with a hidden layer composed of two neurons. The input space is the same used for the previous models.

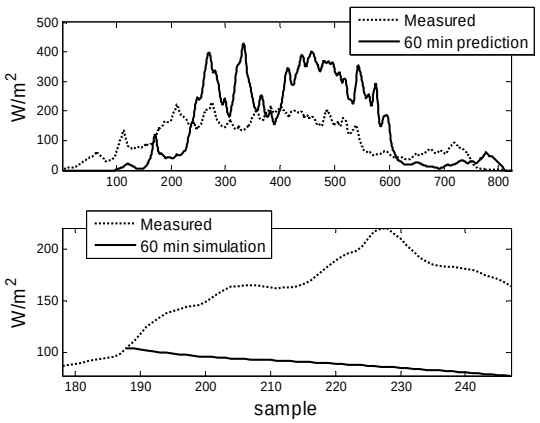

Fig. 14. Top: sixty steps ahead prediction of the solar radiation using an LBN neural network model. Bottom: the prediction tendency in a one hour period taken at sample.

Comparing to the early results, this new prediction tends to overcome the measured radiation. This discrepancy implies a relatively large error. Nevertheless, the dynamic behaviour is, on average, better than the ones achieved with the two previous forecasts methods.

3.3 The Artificial Neural Network (ANN) over Wavelet Decomposition (WD).

The prediction, using this non-linear model architecture was computed by recursion. It's possible to train the network directly for the *k*-step ahead signal. But in this case, the autocorrelation between the present samples and the future ones is to low to belong to the model's input space.

In order to increase the autocorrelation between samples the Haar wavelet is used. A set of ANN will be used to model each of the signals generated by the decomposition. In the end, the partial forecasts are associated in order to produce the final prediction. As before, all the networks will be trained using the last acquired day. The results achieved by this strategy are illustrated in Fig. 15.

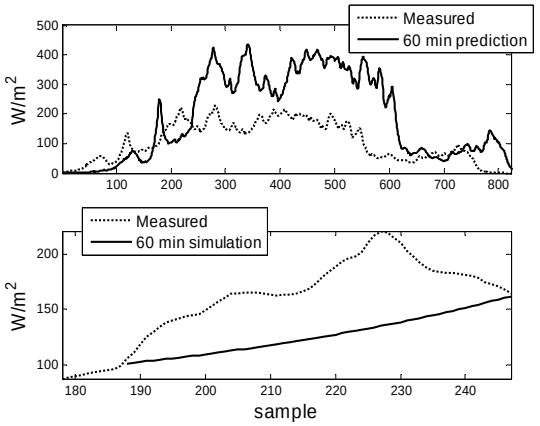

Fig. 15. Top: sixty steps ahead prediction of the solar radiation using an hybrid ANN-WD model. Bottom: the prediction tendency in a one hour period taken at sample.

For the set of running tests, this algorithm has showed the best dynamic forecast behaviour, as seen by the performance indexes (eq. 15 and 16) in table 1. Nevertheless, it was the most complex and time-consuming technique of all.

Table 1 Performance indexes of the four models

Method	J	Q	CE‡/%
AR(10)	31.96	23.37	<7
AR(10)†	47.93	23.88	16
ANN	37.95	31.51	28
ANN-WD	31.44	34.60	100

†Recursive least squares with a 0.998 forgetting factor.
‡Relative computation effort.

#

4. CONCLUSION

In this work several models were tested in order to close predict the solar radiation within a time horizon of one hour. The results reveal better results for non-linear models when compared to linear ones. But it's complexity is, by far, larger and more sensitive to several tuning parameters. On the other hand, the wavelet decomposition has shown an improvement in relation to ANN. More research effort will follow this line of work in the nearby future, with the goal of employing this technique in the prediction of the solar radiation within a greenhouse MBPC- Model Based Predictive Controller.

#

REFERENCES

Coelho, J.P., Moura Oliveira, P.B., Boaventura Cunha, J. (2005). Greenhouse air temperature predictive control using the particle swarm optimisation algorithm. *Computers and Electronics in Agriculture*, Vol. 49, 330-344.

Ferreira, P.M. and A.B. Ruano (2004). Predicting solar radiation with RBF neural networks. 13th C'2004.

Kingdon, J. (1993). Neural nets for time series forecasting: criteria for performance with application in gilt futures pricing. Proc. Neural Networks in Capital Markets.

Mellit, A., M. Benghanem, S.A. Kalogirou (2006). An adaptive wavelet-network model for forecasting daily total solar-radiation. *Applied Energy*, **Vol. 83**, 705-722.

Pedersen, M.W. (1994),. Optimization of recurrent neural networks for time series modelling. PhD Thesis, Lyngby, IMM

Soltani, S. (2002). On the use of the wavelet decomposition for time series prediction. *Neurocomputing* 48. 267–277

Strang, G., T. Nguyen. (1996). *Wavelets and Filter Banks*. Wellesley Cambridge.

van Straten, G. (1996). On-line optimal control of greenhouse crop cultivation. *Acta Hort.* (ISHS), 406:203-212.

Walker, J.S. (1999).*A Primer on Wavelets and their Scientific Applications*. Chapman and Hall/CRC.